Journal of Biomechanics ▮ (▮▮▮▮) ▮▮▮–▮▮▮

Contents lists available at SciVerse ScienceDirect

Journal of Biomechanics

journal homepage: www.elsevier.com/locate/jbiomech
www.JBiomech.com

Biomechanics of the ankle–foot system during stair ambulation: Implications for design of advanced ankle–foot prostheses ☆

Emily H. Sinitski [a], Andrew H. Hansen [b,c], Jason M. Wilken [a,*]

[a] Military Performance Laboratory, Center for the Intrepid, Department of Orthopedics and Rehabilitation, Brooke Army Medical Center, Fort Sam Houston, TX, USA
[b] Minneapolis VA Health Care System, Minneapolis, MN, USA
[c] Department of Physical Medicine and Rehabilitation, Northwestern University Feinberg School of Medicine

ARTICLE INFO

Article history:
Accepted 5 November 2011

Keywords:
Ankle
Foot
Level
Stairs
Prosthesis

ABSTRACT

Unilateral lower limb prosthesis users display temporal, kinematic, and kinetic asymmetries between limbs while ascending and descending stairs. These asymmetries are due, in part, to the inability of current prosthetic devices to effectively mimic normal ankle function. The purpose of this study was to provide a comprehensive set of biomechanical data for able-bodied and unilateral transtibial amputee (TTA) ankle–foot systems for level-ground (LG), stair ascent (SA), and stair descent (SD), and to characterize deviations from normal performance associated with prosthesis use. Ankle joint kinematics, kinetics, torque–angle curves, and effective shapes were calculated for twelve able-bodied individuals and twelve individuals with TTA. The data from this study demonstrated the prosthetic limb can more effectively mimic the range of motion and power output of a normal ankle–foot during LG compared to SA and SD. There were larger differences between the prosthetic and able-bodied limbs during SA and SD, most evident in the torque–angle curves and effective shapes. These data can be used by persons designing ankle–foot prostheses and provide comparative data for assessment of future ankle–foot prosthesis designs.

Published by Elsevier Ltd.

1. Introduction

Unilateral lower limb prosthesis users display temporal (Torburn et al., 1994; Powers et al., 1997), kinematic (Schmalz et al., 2007; Alimusaj et al., 2009), and kinetic (Schmalz et al., 2007; Yack et al., 1999; Alimusaj et al., 2009) asymmetries between limbs during stair ascent (SA) and stair descent (SD). A likely contributor to the asymmetries observed during stair ambulation following unilateral amputation is the lack of a biomimetic (human-like) ankle–foot system. Ankle function during the stance phase can be divided into sub phases to describe different mechanical functions of the ankle including controlled dorsiflexion and plantarflexion, and powered dorsiflexion and plantarflexion (Palmer, 2002; Gates, 2004; Au et al., 2008). Gates (2004) used these phases and calculated ankle torque versus ankle angle (torque–angle) curves to demonstrate distinct mechanical requirements of the able-bodied human ankle between level-ground (LG), SA, and SD walking.

The torque–angle curve has been used by a number of investigators to examine the biomechanics of the ankle during LG walking (Mesplay, 1993; Davis and DeLuca, 1996; Palmer, 2002; Hansen et al., 2004a). The slope of the torque–angle curve can provide an indication of torsional stiffness that could be used to mimic the behavior of the human ankle in a prosthesis. However, the slope should be thought of as "quasi-stiffness" since the measurements are not performed at equilibrium (Latash and Zatsiorsky, 1993). To our knowledge, Gates (2004) is the only investigator who has used torque-angle curves to examine stair ambulation in able-bodied individuals, but the investigation did not include individuals using lower limb prostheses.

Classical gait analysis (i.e. kinematics and kinetics plotted as a function of time or gait cycle) and ankle torque–angle curves provide a wealth of information to persons designing prosthetic ankle–foot systems. However, these data still lack information regarding the actual movements and deformations within the foot due to rigid body assumptions. The effective shape is a relatively new approach for characterizing the function of the ankle–foot complex. The effective shape of the ankle–foot is determined by calculating the center of pressure (COP) position in a shank-based local coordinate system. In physiologic systems,

☆ The view(s) expressed herein are those of the author(s) and do not reflect the official policy or position of Brooke Army Medical Center, the U.S. Army Medical Department, the U.S. Army Office of the Surgeon General, the Department of the Army, Department of Defense, Department of Veterans Affairs, or the U.S. Government.

* Corresponding author. Tel.: +210 916 1478; fax: +210 916 9016.
E-mail addresses: Jason.Wilken@us.army.mil, jason.wilken@gmail.com (J.M. Wilken).

0021-9290/$ - see front matter Published by Elsevier Ltd.
doi:10.1016/j.jbiomech.2011.11.007

Report Documentation Page

Form Approved
OMB No. 0704-0188

1. REPORT DATE	2. REPORT TYPE	3. DATES COVERED
15 DEC 2011		**00-00-2011 to 00-00-2011**

4. TITLE AND SUBTITLE	5a. CONTRACT NUMBER
Biomechanics Of The Ankle-Foot System During Stair Ambulation: Implications For Design Of Advanced Ankle-Foot Prostheses	5b. GRANT NUMBER
	5c. PROGRAM ELEMENT NUMBER
6. AUTHOR(S)	5d. PROJECT NUMBER
	5e. TASK NUMBER
	5f. WORK UNIT NUMBER
7. PERFORMING ORGANIZATION NAME(S) AND ADDRESS(ES) **Brooke Army Medical Center,Military Performance Laboratory,Fort Sam Houston,TX,78234**	8. PERFORMING ORGANIZATION REPORT NUMBER
9. SPONSORING/MONITORING AGENCY NAME(S) AND ADDRESS(ES)	10. SPONSOR/MONITOR'S ACRONYM(S)
	11. SPONSOR/MONITOR'S REPORT NUMBER(S)

12. DISTRIBUTION/AVAILABILITY STATEMENT
Approved for public release; distribution unlimited

13. SUPPLEMENTARY NOTES
Journal of Biomechanics, preprint, 15 December 2011

14. ABSTRACT

15. SUBJECT TERMS

16. SECURITY CLASSIFICATION OF:			17. LIMITATION OF ABSTRACT	18. NUMBER OF PAGES	19a. NAME OF RESPONSIBLE PERSON
a. REPORT	b. ABSTRACT	c. THIS PAGE			
unclassified	**unclassified**	**unclassified**	**Same as Report (SAR)**	**8**	

the effective shape captures contributions of tissue deformation as well as joint movements at the ankle and foot to provide a net output of the ankle–foot system. The effective shape during LG has been referred to as a "roll-over shape" and is consistent when able-bodied persons walk at different speeds (Hansen and Childress, 2004), carry additional weight (Hansen and Childress, 2005), or walk with shoes of different heel heights (Hansen and Childress, 2004) or rocker radii (Wang and Hansen, 2010). These shapes also change significantly for ramp walking (Hansen et al., 2004b) in a way that suggests the need for different prosthetic alignment (e.g. dorsiflexed alignment for uphill walking). Mimicking the effective shape of the intact ankle–foot system can be used as a criterion for prostheses design (Sam et al., 2004). However, effective shapes have not been used to examine biomechanics of able-bodied or prosthetic ankle–foot systems during stair ambulation.

The purpose of this study was to present a comprehensive set of biomechanical data for able-bodied ankle–foot systems for LG, SA, and SD, and to determine where significant deviations from able-bodied performance exist during ambulation with a prosthesis following unilateral transtibial amputation (TTA). Specifically, we calculated the kinematics and kinetics, torque-angle curves, and effective shapes during walking in each condition for a single cohort of subjects. We hypothesized the prosthetic limb would differ significantly from able-bodied data across all measures, and the intact limb would demonstrate compensatory motion and loading due to deficiencies in the prosthetic limb. We also hypothesized current prosthetic devices provide more biomimetic function for LG walking compared with SA and SD. These data can be used by persons designing ankle–foot prostheses and provide comparative data for assessment of future ankle–foot prosthesis designs.

2. Methods

See Supplemental material for detailed description of all methodologies.

2.1. Subjects

Twelve individuals (11 males and 1 female; mass = 87 ± 10 kg; height = 1.8 ± 0.1 m; age = 28 ± 6 yrs.) with unilateral traumatic transtibial amputation and no co-morbidities to the intact limb volunteered to participate in this study (Supplemental Table S1). This population is representative of injured military service members and is similar to the general population of young males (Stinner, Burns et al., 2010). Twelve gender, height, and weight matched able-bodied individuals (11 males and 1 female; mass = 87 ± 12 kg; height = 1.8 ± 0.1 m; age = 23 ± 5 yrs.) with no current pain or history of major lower extremity injury also volunteered to participate in this study. This study was approved by the Institutional Review Board at Brooke Army Medical Center, Ft. Sam Houston, TX, and all participants provided written, informed consent prior to participation.

2.2. Collection methodology

All subjects underwent a single biomechanical gait assessment while walking on level-ground, and up and down a custom 16-step instrumented staircase (Supplemental Fig. S1). An auditory cue was provided to guide subjects to walk at a controlled speed normalized to leg length (Hof, 1996) during level-ground (LG) or a controlled cadence of 80 steps per minute during stair ascent (SA) and stair descent (SD) (Wilken, Sinitski et al., 2011). Full body kinematics (Supplemental Fig. S2) were collected at 120 Hz using a 26 camera motion capture system (Motion Analysis Corp., Santa Rosa, CA). Motion of the foot and tibia were tracked based on Manal et al. (2002) and Collins et al. (2009), and the segment coordinate systems were defined using ISB recommendations (Wu, Siegler et al., 2002). Kinetics were collected at 1200 Hz using two force plates (AMTI, Inc., Watertown, MA) and were synchronized with kinematic data. Five trials for LG, SA, and SD were analyzed using Visual3D (C-Motion Inc., Germantown, MD) and MATLAB (The Mathworks, Natick, MA) software.

2.3. Kinematic and kinetic analysis

Using Visual3D, ankle motion was calculated by comparing the orientation of the foot and tibial local coordinate systems using an Euler angle approach, and ankle joint moments were calculated using inverse dynamics and resolved in the tibial coordinate system. Calculated ankle joint motion, joint moment, and joint power were time normalized to 0–100% of the gait cycle and were assessed at several points in the gait cycle.

2.4. Torque–angle analysis

To quantify differences between torque–angle (ankle moment versus ankle angle) curves, work was estimated by determining the area under the torque–angle curve using a trapezoidal approximation. The work for each ankle function phase during stance was estimated (controlled plantarflexion, controlled dorsiflexion, and powered plantarflexion), and the total work during stance was calculated as the sum of these phases.

2.5. Ankle–foot effective shape analysis

The effective shapes of the ankle–foot system during LG, SA, and SD walking were calculated for the stance cycle using previously described methods for level walking roll-over shapes (Fatone and Hansen, 2007), and is described in more detail in the Supplemental material. Effective shapes for the stance cycle were determined by calculating the location of COP in the shank-based coordinate system (Supplemental Fig. S3). To quantify the differences between tasks, the average distance (mean distance) between the stair effective shape (SA or SD) and the LG effective shape was calculated over the step cycle (Supplemental Fig. S4).

2.6. Statistical analysis

All statistical analyses were performed using SPSS 16 (SPSS Inc, Chicago), with a level of significance of $p \leq 0.05$ for all comparisons. One-way ANOVAs were used to identify kinematic and kinetic differences between limbs (able-bodied, intact, and prosthetic). A two-way ANOVA was used to identify ankle range-of-motion differences between walking conditions (LG, SA, and SD) and limbs. A two-way ANOVA was also used to identify differences in total work (torque–angle) and mean distance (effective shape) between walking conditions (LG, SA, and SD) and limbs (able-bodied, intact, and prosthetic). Significant interaction effects for the one-way ANOVAs were explored using a Tukey test and a Sidak correction was used to determine significant interaction for two-way ANOVAs.

3. Results

Group mean ± standard deviation (sd) for each parameter are presented in Table 1 and detailed results from all statistical analyses are presented in the Supplemental material (Supplemental Table S2). There were significant limb main effects for all kinematic parameters during stance ($p < 0.01$; Fig. 1A, top row). Ankle range-of-motion (ROM) also demonstrated significant main effects for walking condition (LG, SA, and SD) ($p < 0.001$; Fig. 1A, top row). There were significant limb main effects for all kinetic parameters during stance ($p < 0.025$; Fig. 1A, middle and bottom row) with the exception of peak power absorption during mid-stance and peak plantarflexor moment during late stance during LG ($p > 0.4$), and peak plantarflexor moment during early stance during SD ($p > 0.1$).

Ensemble average torque–angle curves for all limb and walking conditions are shown in Fig. 1B where initial contact is depicted by a circle, and the stance phase is divided into a thick line (initial contact to opposite initial contact) and thin line (opposite initial contact to toe-off).

The resulting mean effective shapes during LG, SA, and SD for all subjects are shown in Fig. 1C and these same mean effective shapes are presented by limb (able-bodied, intact, and prosthetic) in Fig. 1D. For able-bodied and intact limbs the LG effective shape curves in a superior direction as the COP moves anteriorly from the heel to the toe during the stance phase (Fig. 1C, left column). Unlike LG, the COP during SA remains on the forefoot during stance resulting in an effective shape clustered anterior to the ankle joint center (Fig. 1C, middle column). The effective shape during SA migrates superiorly and posteriorly as the foot is loaded and ankle moves into dorsiflexion. Then the effective shape moves in a downward direction as the foot moves into

Please cite this article as: Sinitski, E.H., et al., Biomechanics of the ankle–foot system during stair ambulation: Implications for design of advanced ankle–foot prostheses. Journal of Biomechanics (2011), doi:10.1016/j.jbiomech.2011.11.007

Table 1
Mean and standard deviations across subjects for each walking condition (level-ground, stair ascent, and stair descent) and limb condition (able-bodied, intact, and prosthetic).

Kinematics and kinetics			Able-bodied		Intact		Prosthetic	
			Mean	sd	Mean	sd	Mean	sd
Level-ground								
Ankle range-of-motion	(deg)	† * □	29.02	4.09	30.23	3.15	19.89	3.75
Plantarflexion during early stance	(deg)	†	−6.21	2.61	−3.63	2.49	−1.30	3.28
Dorsiflexion during stance	(deg)	†	14.94	2.87	15.95	3.06	18.59	2.61
Dorsiflexor moment during early stance	(N/kg)	†	−0.26	0.06	−0.26	0.05	−0.32	0.07
Plantarflexor moment during late stance	(N/kg)		1.42	0.12	1.39	0.16	1.34	0.17
Power absorption during mid-late stance	(W/kg)		−1.02	0.30	−1.02	0.38	−1.07	0.35
Power generation during late stance	(W/kg)	†	2.54	0.57	2.42	0.31	1.52	0.33
Stair ascent								
Ankle range-of-motion	(deg)	† * □	42.21	5.11	51.76	4.73	9.72	2.27
Dorsiflexion during stance	(deg)	†	23.41	2.61	26.77	2.92	15.57	3.30
Plantarflexion during late stance	(deg)	†	18.74	5.15	24.98	5.43	5.96	2.31
Plantarflexor moment during late stance	(N/kg)	†	1.25	0.13	1.43	0.27	1.02	0.22
Power generation during late stance	(W/kg)	†	2.56	0.59	4.26	1.31	0.77	0.33
Stair descent								
Ankle range-of-motion	(deg)	† * □	60.84	3.68	66.07	4.60	11.39	3.50
Plantarflexion during early stance	(deg)	†	25.11	2.92	29.10	4.11	3.76	3.45
Dorsiflexion during stance	(deg)	†	33.45	4.95	34.75	4.07	14.91	3.47
Plantarflexor moment during early stance	(N/kg)		1.03	0.15	1.16	0.32	0.97	0.24
Power absorption during early stance	(W/kg)	†	−3.01	0.59	−5.98	2.04	−0.40	0.27
Power generation during late stance	(W/kg)	†	1.38	0.36	1.58	0.36	0.56	0.29
Total work								
Level-ground	Nm · deg/kg	† * □	1.4	2.8	2.9	2.3	−5.2	2.8
Stair ascent	Nm · deg/kg	† * □	22.1	6.2	32.6	7.3	−0.6	0.6
Stair descent	Nm · deg/kg	† * □	−32.0	4.6	−38.3	10.6	−2.4	1.9
Mean distance (effective shape)								
Stair ascent	(cm)	† * □	3.1	0.4	6.3	2.1	2.6	1.1
Stair descent	(cm)	† * □	6.5	0.9	9.3	1.5	1.7	0.9

† significant main effect for limb.
* significant main effect for condition.
□ significant limb × condition interaction ($p \leq 0.05$).

plantarflexion. In contrast, the effective shape during SD begins considerably below the LG effective shape and anterior to the ankle joint center (Fig. 1C, right column). During the initial lowering phase of SD, as the forefoot is loaded, the effective shape progresses superiorly. After the foot is flat on the step, the effective shape travels superiorly and anteriorly as weight is shifted further onto the forefoot as the ankle moves into dorsiflexion.

Ankle function can be described by dividing the stance phase into controlled dorsiflexion (CD) and plantarflexion (CP), and powered dorsiflexion (PD) and plantarflexion (PP) (Palmer, 2002; Gates, 2004; Au, Berniker et al., 2008). The ankle function phases for LG, SA, and SD and the corresponding work for each of these phases is presented in Fig. 2. Controlled ankle motion is indicated by net negative work occurring over an interval and powered ankle motion is indicated by net positive work occurring over an interval. There were significant interaction effects (limb*condition) for total work at the ankle ($p < 0.001$; Fig. 3). Separate one-way ANOVAs were used to explore limb and condition pairwise comparisons using a Tukey correction. Able-bodied and intact limbs exhibited significant differences between LG, SA, and SD ($p < 0.001$). The prosthetic limb was only significantly different between LG and both SA and SD ($p < 0.006$). During LG and SD, the total work at the ankle was not significantly different for able-bodied and intact limbs ($p > 0.07$), but these limbs were significantly different than the prosthetic limb ($p < 0.001$). During SA, all limb conditions were significantly different ($p < 0.001$).

There were significant limb, walking condition, and interaction effects for distance between the LG effective shape and the stair effective shape (SA or SD) ($p < 0.001$; Fig. 4). For both walking conditions (SA and SD), the distance between effective shapes were significantly different for all limb comparisons ($p < 0.001$) except between able-bodied and prosthetic during SA ($p > 0.6$). Both able-bodied and intact limbs exhibited significant differences between SA and SD ($p < 0.001$), and the prosthetic limb showed no significant differences between SA and SD ($p > 0.1$).

4. Discussion

This study is the first to examine conventional kinematic and kinetic data, torque–angle, and effective shape data of the ankle–foot system, including ensemble average data, for able-bodied individuals and individuals with unilateral transtibial amputation during level-ground (LG), stair ascent (SA), and stair descent (SD) walking. Overall, the prosthetic limb is able to replicate the physiologic ankle–foot system for much of the gait cycle during LG walking, but does not effectively mimic the physiologic ankle–foot system during SA or SD. The ankle–foot biomechanical data presented in able-bodied individuals and individuals with TTA during stair ambulation can be used to guide development of biomimetic foot and ankle prosthetic devices.

4.1. Level-ground

Conventional energy storing and return prosthetic feet (ESR) can mimic able-bodied ankle–foot function during most of the stance phase (Hansen, Childress et al., 2000). Fig. 1A demonstrates the

Please cite this article as: Sinitski, E.H., et al., Biomechanics of the ankle–foot system during stair ambulation: Implications for design of advanced ankle–foot prostheses. Journal of Biomechanics (2011), doi:10.1016/j.jbiomech.2011.11.007

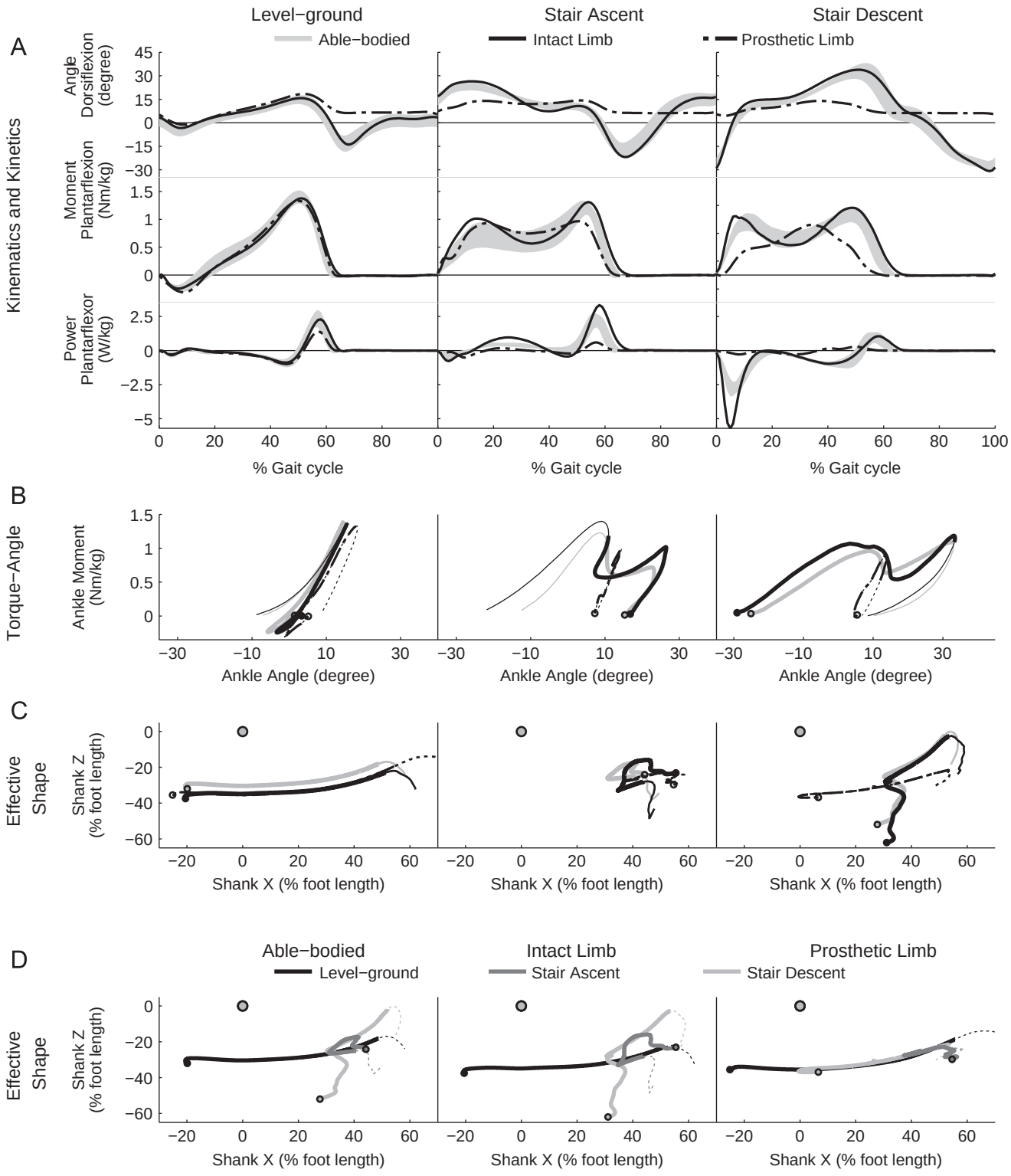

Fig. 1. (A) Ankle kinematics and kinetics for level-ground (LG), stair ascent (SA), and stair descent (SD) walking. The gray band represents the mean ± standard deviation (sd) of the able-bodied subjects, the black solid line represents the mean of the intact limb, and the black dashed line represents the mean of the prosthetic limb. (B) Mean torque-angle (ankle moment versus ankle angle) curves during LG, SA, and SD walking. The gray line represents the mean of able-bodied subjects, the black solid line represents the mean of the intact limb, and the black dashed line represents the mean of the prosthetic limb. Heel contact is indicated by a circle. The thicker line on each torque-angle curve represents the step cycle and the thinner line represents the remainder of stance equivalent to terminal double support. (C) Mean effective shape during LG, SA, and SD walking. The gray line represents the mean of able-bodied subjects, the black solid line represents the mean of the intact limb, and the black dashed line represents the mean of the prosthetic limb. Heel contact is indicated by a circle. The thicker line on each effective shape represents the step cycle and the thinner line represents the remainder of stance equivalent to terminal double support. The circle plotted at (0, 0) represents the ankle joint center. (D) The same mean effective shapes from C plotted by limb condition (normal, intact, and prosthetic). The black line represents the LG effective shape, the dark gray line represents the SA effective shape, and the light gray line represents the SD effective shape. Heel contact is indicated by a circle. The solid line on each effective shape represents the step cycle and the dotted line represents the remainder of stance equivalent to terminal double support. The circle plotted at (0, 0) represents the ankle joint center.

Please cite this article as: Sinitski, E.H., et al., Biomechanics of the ankle–foot system during stair ambulation: Implications for design of advanced ankle–foot prostheses. Journal of Biomechanics (2011), doi:10.1016/j.jbiomech.2011.11.007

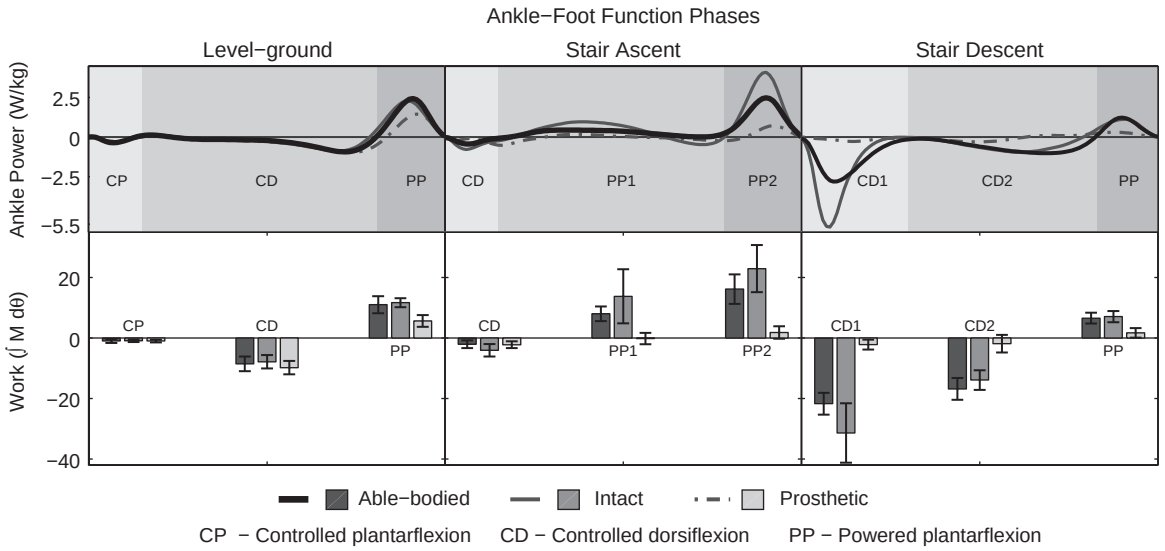

Fig. 2. Ankle–foot function during the stance phase for level-ground (LG), stair ascent (SA), and stair descent (SD). The top row displays mean ankle power for each walking condition and limb, where the thick black line represents the mean of the able-bodied subjects, the gray solid line represents the mean of the intact limb, and the gray dashed line represents the mean of the prosthetic limb. The bottom row displays the net work for each of these phases. Controlled ankle function is indicated by net negative work and powered ankle function is indicated by net positive work.

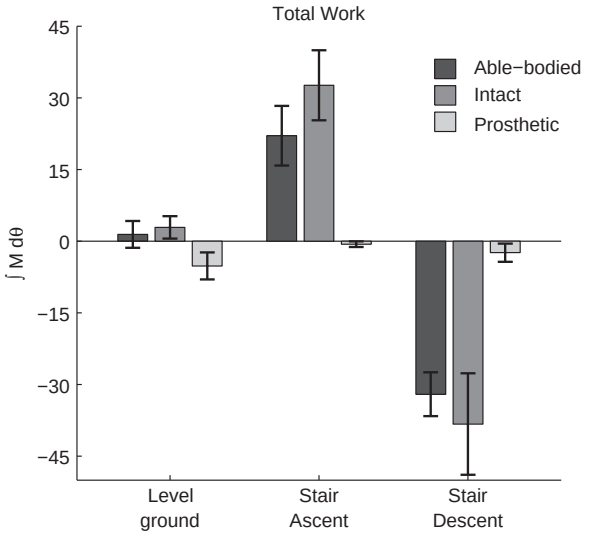

Fig. 3. Total work (mean ± sd) at the ankle for level-ground (LG), stair ascent (SA), and stair descent (SD) walking. Between limb differences were only observed between the prosthetic limb and both able-bodied and intact limbs for LG and SD walking conditions ($p < 0.001$). During SA all between limb comparisons were significant ($p < 0.001$). Able-bodied and intact limbs exhibited between walking condition (LG, SA, and SD) differences for all comparisons ($p < 0.001$). In the prosthetic limb, between walking condition differences were only observed between LG and both SA and SD ($p < 0.006$).

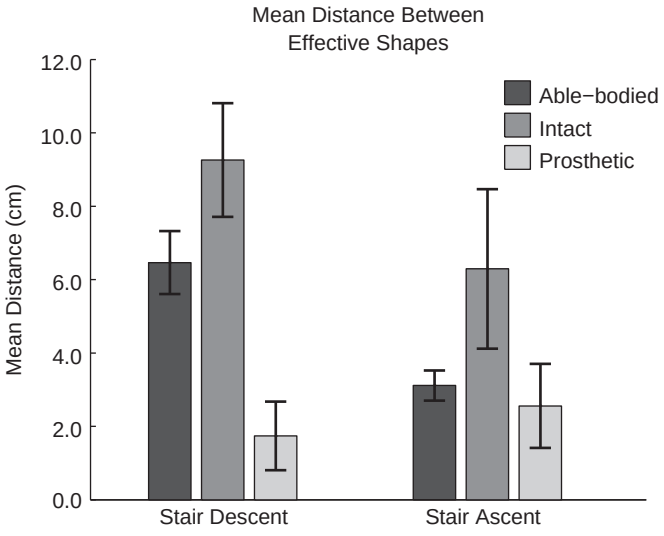

Fig. 4. Mean distance (mean ± sd) between the level effective shape and stair effective shape (SA or SD) for each limb condition (able-bodied, intact, and prosthetic). Between limb comparisons for both SA and SD were statistically significant ($p < 0.001$) with the exception of the able-bodied and prosthetic limb comparison during stair ascent ($p > 0.6$). Between walking condition comparisons were statistically significant ($p < 0.001$) for both able-bodied and intact limbs ($p < 0.001$), but not for the prosthetic limb ($p > 0.1$).

prosthetic limb has similar ankle motion, moment, and power during controlled plantarflexion (CP) and controlled dorsiflexion (CD) compared to the able-bodied ankle–foot. Futhermore, the prosthetic limb also produces a similar torque–angle curve (Fig. 1B) and effective shape (Fig. 1C) during these phases compared to the able-bodied ankle–foot. However, during the powered plantarflexion (PP) period of the stance phase, ESR do not provide plantarflexion and can only return to neutral as they are unloaded. As a result, the prosthetic limb produces significantly less power, which is evident in the torque–angle curves and corresponding negative total work over the stance cycle. The effective shape also reflects the lack of plantarflexion exhibiting a roll-off rather than a push-off pattern (Fig. 1C). During late stance, the intact limb plantarflexes producing a rapid lowering of the COP whereas in the prosthetic foot, the COP moves further anteriorly rolling off the toe as the foot is unloaded and returns to a neutral position. Although ESR do not provide powered plantarflexion during late stance, the total work required for an able-bodied ankle–foot is small during LG walking, and a prosthetic limb is able to approximate able-bodied ankle–foot function.

4.2. Stair ascent

The able-bodied ankle–foot system requires greater ankle ROM, torque, and power during SA compared to LG. The

Please cite this article as: Sinitski, E.H., et al., Biomechanics of the ankle–foot system during stair ambulation: Implications for design of advanced ankle–foot prostheses. Journal of Biomechanics (2011), doi:10.1016/j.jbiomech.2011.11.007

prosthetic limb only maintains a slightly dorsiflexed position during mid-stance (PP1) and is able to approximate able-bodied torque during controlled dorsiflexion (CD), but lacks able-bodied plantarflexion motion. Additionally, the prosthetic limb is not able to produce plantarflexion motion and the associated power output required during late stance (PP2). This is evident in the torque–angle curve (Fig. 1B), effective shape (Fig. 1C), and the large difference in total work at the ankle (Fig. 3). Prosthetic feet deform to provide limited dorsiflexion and both the torque–angle curve and effective shape clearly illustrate how the lack of ankle ROM limits the ankle–foot function during SA. Able-bodied individuals place their foot on the step in greater ankle dorsiflexion than LG with their tibia positioned forward. In individuals with TTA it is more challenging to transition over the prosthetic limb due to a decrease in ankle dorsiflexion during early stance, and the intact limb compensates by increasing plantarflexion during late stance. Furthermore, the intact limb increases the total work (Fig. 3) and alters the torque–angle curve (Fig. 1B) and effective shape (Fig. 1C) to compensate for the impaired function of the prosthetic limb. A prosthetic foot aligned in more dorsiflexion is believed to allow the amputee to walk up stairs more easily (Alimusaj et al., 2009). However, during SA there is not a "roll-over" observed during LG. Although a more dorsiflexed position may make it easier to transition onto the prosthetic limb, the torque–angle curve demonstrates limited energy storage and return in the prosthesis (Fig. 1C), and an increased dorsiflexed alignment further reduces an already limited energy return (Alimusaj et al., 2009). Recent findings suggest the importance of ankle power in the vertical acceleration of the body during late stance of the SA gait cycle (Wilken et al., 2011). The approach of using fixed offsets in alignment of prosthetic feet during SA may reduce energy return and have unintended negative consequences.

4.3. Stair descent

Similar to SA, the prosthetic limb does not effectively mimic able-bodied ankle–foot function during SD and demonstrates the largest differences between prosthetic limb and intact limb. The able-bodied ankle–foot system requires greater ROM during SD compared to LG and SA. The prosthetic limb only allows a slightly dorsiflexed position during stance (CD1 and CD2) and does not provide plantarflexion motion and the associated power absorption during early stance (CD1). These limitations are evident in the torque–angle curve (Fig. 1B), effective shape (Fig. 1C), and the large difference in total work at the ankle (Fig. 3). Prior to initial contact, able-bodied individuals plantarflex their foot and make initial contact with the forefoot on the step. In the prosthetic limb, there is no plantarflexion and as a result the prosthetic limb makes a heel or flatfoot initial contact (Fig. 1A). This lack of plantarflexion in early stance leads to rolling movement during stance similar to LG, which is observed in the effective shape (Fig. 1C). Able-bodied individuals continually dorsiflex the ankle during stance controlling the descent of the body to the next step. Due to limited dorsiflexion motion in the prosthetic limb, individuals with amputation have increased difficulty with weight transfer and often "fall" onto their intact limb (Schmalz et al., 2007) resulting in larger peak ankle power absorption (Fig. 1A) and negative work (Fig. 3). Alimusaj (2009) reported an adaptive ankle allowing approximately 5° more dorsiflexion, significantly reduced peak ankle power absorption on the intact limb. Although pre-positioning the ankle in more dorsiflexion may be beneficial during late stance, the power absorption on the intact limb remains nearly 1.5 × greater than observed in able-bodied individuals (Alimusaj, Fradet et al., 2009; Table 2).

5. Conclusions

Conventional prosthetic feet allow individuals with lower extremity amputation to return to many functional activities; however these passive prosthetic feet do not fully replicate mechanical characteristics of the able-bodied ankle–foot system. The prosthetic limb is able to better mimic the range of motion and power output of an able-bodied ankle–foot system during LG compared to SA and SD. There are still limitations with a prosthetic limb, specifically during SA and SD, demonstrated by the larger differences in torque–angle curves and effective shapes. Currently, there are adaptable ankle–foot prostheses available that pre-position the ankle in dorsiflexion (i.e. Propio-Foot$_{TM}$, Ossur), but this method only provides subtle improvements in gait for individuals with lower extremity amputation (Alimusaj, Fradet et al., 2009). Substantial improvements can only be obtained by addressing the fundamental limitations of passive prosthetics. Studies are currently underway to determine the ability of next generation powered prosthetic technologies to effectively replicate able-bodied function and overcome limitations of conventional ESR feet. The data presented in this paper are intended to aid prosthetic device designers to develop passive or active solutions to effectively mimic able-bodied ankle–foot mechanical characteristics.

Conflict of Interest

The authors declare there is no conflict of interest associated with this work.

Acknowledgments

This study was funded in part by grants from the Military Amputee Research Program (to JMW) and the Telemedicine and Advanced Technology Research Center (to JMW) and was supported by the Department of Veterans Affairs, Veterans Health Administration, Rehabilitation Research and Development Service (AHH). The authors would like to thank Jennifer Aldridge, Kelly Rodriguez, and Linda Waetjen for their contributions to data collection and processing.

Appendix A. Supporting materials

Supplementary data associated with this article can be found in the online version at doi:10.1016/j.jbiomech.2011.11.007.

References

Alimusaj, M., Fradet, L., et al., 2009. Kinematics and kinetics with an adaptive ankle–foot system during stair ambulation of transtibial amputees. Gait and Posture 30 (3), 356–363.

Au, S., Berniker, M., et al., 2008. Powered ankle–foot prosthesis to assist level-ground and stair-descent gaits. Neural Network 21 (4), 654–666.

Collins, T.D., Ghoussayni, S.N., et al., 2009. A six degrees-of-freedom marker set for gait analysis: repeatability and comparison with a modified Helen Hayes set. Gait and Posture 30 (2), 173–180.

Davis, R., DeLuca, P., 1996. Gait characterization via dynamic joint stiffness. Gait and Posture 4 (3), 224–231.

Fatone, S., Hansen, A.H., 2007. Effect of ankle–foot orthosis on roll-over shape in adults with hemiplegia. Journal of Rehabilitation Research and Development 44 (1), 11–20.

Gates, D.H., 2004. Characterizing Ankle Function During Stair Ascent, Descent, And Level Walking For Ankle Prosthesis And Orthosis Design. M.S. Thesis.

Hansen, A.H., Childress, D.S., 2004. Effects of shoe heel height on biologic rollover characteristics during walking. Journal of Rehabilitation Research and Development 41 (4), 547–554.

Hansen, A.H., Childress, D.S., 2005. Effects of adding weight to the torso on roll-over characteristics of walking. Journal of Rehabilitation Research and Development 42 (3), 381–390.
Hansen, A.H., Childress, D.S., et al., 2000. Prosthetic foot roll-over shapes with implications for alignment of trans-tibial prostheses. Prosthetics and Orthotics International 24 (3), 205–215.
Hansen, A.H., Childress, D.S., et al., 2004a. Roll-over shapes of human locomotor systems: effects of walking speed. Clinical Biomechanics 19 (4), 407–414.
Hansen, A.H., Childress, D.S., et al., 2004b. Roll-over characteristics of human walking on inclined surfaces. Human Movement Science 23 (6), 807–821.
Hof, A.L., 1996. Scaling gait data to body size. Gait and Posture 4, 222–223.
Latash, M.L., Zatsiorsky, V.M., 1993. Joint stiffness: myth or reality? Human Movement Science 12, 653–692.
Manal, K., McClay, I., et al., 2002. Knee moment profiles during walking: errors due to soft tissue movement of the shank and the influence of the reference coordinate system. Gait and Posture 15 (1), 10–17.
Mesplay, K., 1993. Mechanical Impedance of the Human Lower Limb During Walking. Ph.D. Thesis.
Palmer, M., 2002. Sagittal Plane Charaterization Of Normal Human Ankle Function Across A Range Of Walking Gait Speeds. M.S. Thesis. Massachusetts Institute of Technology, Cambridge.
Powers, C.M., Boyd, L.A., et al., 1997. Stair ambulation in persons with transtibial amputation: an analysis of the Seattle LightFoot. Journal of Rehabilitation Research and Development 34 (1), 9–18.
Sam, M., Childress, D.S., et al., 2004. The 'shape&roll' prosthetic foot: I. Design and development of appropriate technology for low-income countries. Medicine, Conflict, and Survival 20 (4), 294–306.
Schmalz, T., Blumentritt, S., et al., 2007. Biomechanical analysis of stair ambulation in lower limb amputees. Gait and Posture 25 (2), 267–278.
Stinner, D.J., Burns, T.C., et al., 2010. Return to duty rate of amputee soldiers in the current conflicts in Afghanistan and Iraq. Journal of Trauma 68 (6), 1476–1479.
Torburn, L., Schweiger, G.P., et al., 1994. Below-knee amputee gait in stair ambulation. A comparison of stride characteristics using five different prosthetic feet. Clinical Orthopaedics and Related Research 303, 185–192.
Wang, C.C., Hansen, A.H., 2010. Response of able-bodied persons to changes in shoe rocker radius during walking: changes in ankle kinematics to maintain a consistent roll-over shape. Journal of Biomechanics 43 (12), 2288–2293.
Wilken, J.M., Sinitski, E.H., et al., 2011. The role of lower extremity joint powers in successful stair ambulation. Gait and Posture.
Wu, G., Siegler, S., et al., 2002. ISB recommendation on definitions of joint coordinate system of various joints for the reporting of human joint motion—part I: ankle, hip, and spine. Journal of Biomechanics 35 (4), 543–548.
Yack, H.J., Nielsen, D.H., et al., 1999. Kinetic patterns during stair ascent in patients with transtibial amputations using three different prostheses. Journal of Prosthetics Orthotics 11 (3), 57–62.

Please cite this article as: Sinitski, E.H., et al., Biomechanics of the ankle–foot system during stair ambulation: Implications for design of advanced ankle–foot prostheses. Journal of Biomechanics (2011), doi:10.1016/j.jbiomech.2011.11.007